

ea e e e a e a e e
ea e a e e a a e e ()
a ea e e e a e a e

†, & ††, †
ee ae e a ee, e, 10003, a
† a e e a ea e e, a 210016, a
ea e e ee, e, , 36 4 -5305,

(Received 1 2015 accepted a a 2016 first published online 1 2016)

ac ee e e ea , aea e e a aa e ee
e e e aea e e ea e a e e a a e
e () ea e a ea e e eea e a eae. e
ae aa eea a e ae e aea e a e a ~4.5 a e
e a e e e e a ~400 a , e a e e e ae e e e
aea e. a e e e e e ae aae e e a
e e - e e. a, e a eea
e ε (t) (13 20) a a e δ¹ (+5.3 ‰) a e e ae a e
ae a e e a a e e a e e e e e a a
e a a e e e ea a e aa e a / - eae . eaa
eee , e e e e , ae a e aea a aa
eae e e e - e, e a ee eea ea - ea e
a ea e a e e e e e e e e e a e, a- ea
e e a e a e a- ca a, a e e eae e ea e
a a- ca a e a e e. eae ae, e aea a a ea ee
ea e a e ea e e e a e e e e - a e
e
e aea e, - e, a e e, e a a e e (),
a eae.

1. I c
e, a e a e e ee e ae ,
eaa a e e
a- ea a e a - e e e
(e. . a et al. 200 e & e, 200 e-
a a et al. 2012 a et al. 2012, 2013 a a
et al. 2013), a a a a a-
a e e ea a e, e ea e
a a e a e e e
e e (, 1 a et al. 200 a et al.
200 a). a a e a ee e e
a e e e e e e e e-
e (e a, 1
a, 1 , 1 3 a a e e et al. 2000 e
& e, 2003 a et al. 200 ea e, 2014).
a ee e e , e & e (2011) a -
e e e a e e e a a-
, - ea e, e, a-
(), a a a a e a .
eee e e e , ea e (2014) e -

e a e, .e. - ea - e e
a - e e. e - ea e e
a e e - e, - ea - e -
e, e e - e e e e e
a - a e, a - a a ea
e-
a e e e e e e e -
e e e a a e e e (),
eae ae a e a e e e
(e ö, aa & a, 1 3 a ,
& e, 2000 e et al. 2002 a et al. 2004,
200 a) (. 1a). eae ee e a e
e a e , a e e -
e e (a et al. 200 a, b e ,
e & a , 2012). ea e a ,
e e a e e e e e e
ea e a e e e e e e e
ea , , e ea e ,
aea a a, a aaaa e e
(a , 1 3 a et al. 2003 a et al.
2003 a et al. 200 a) (. 1). a -
e a e e a e e e e , e e-
ae a a , e e , e e

† e e e a 16 a .

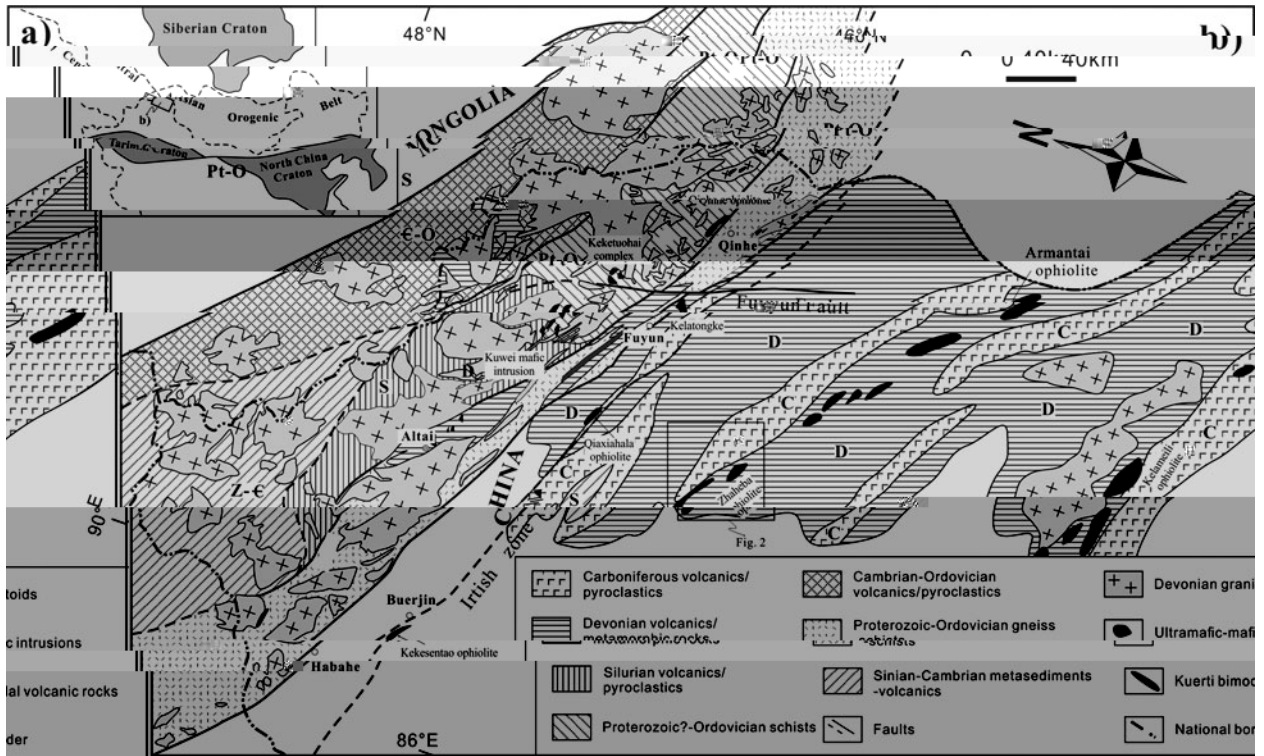


Fig. 1. (a) Geological map of the Altai region in Mongolia and China, showing various tectonic units, faults, and ophiolite belts. (b) Detailed view of the Arantai ophiolite belt. The map includes a legend with symbols for different geological features and a scale bar.

... $> 0\%$... (0.3, ...). ... (1) ... (2) ... (0.3). ...

2. R ... (1, 2). ... (0.3a). ... (0.2). ... (0.2). ... (1, 3).

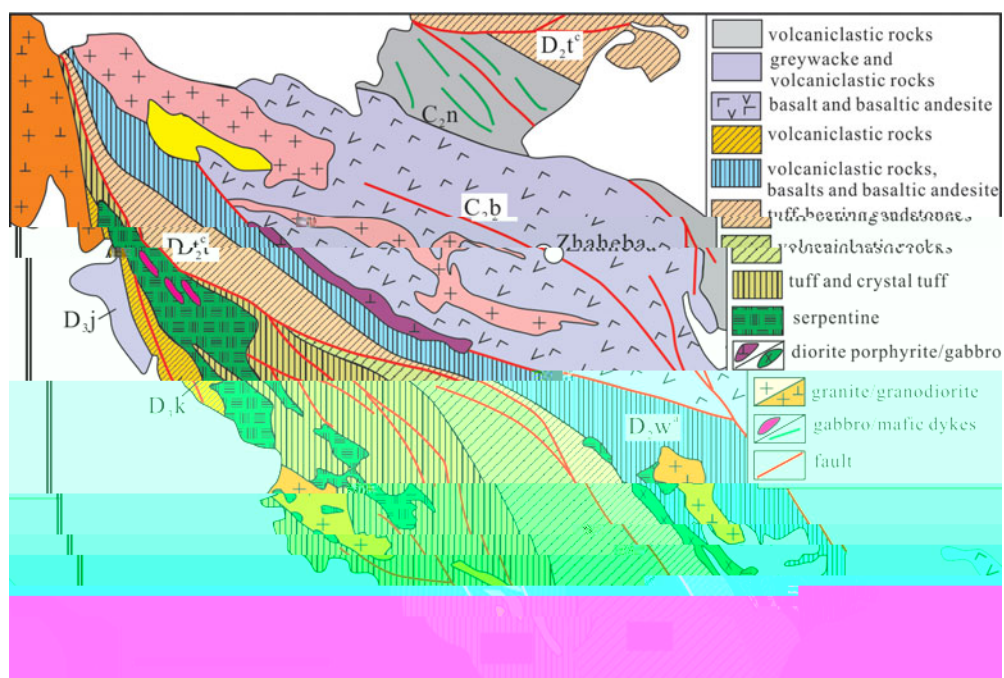


Fig. 2. Geological map of the Zhaheba ophiolite (after Wang et al., 2000, 2001, 2003).

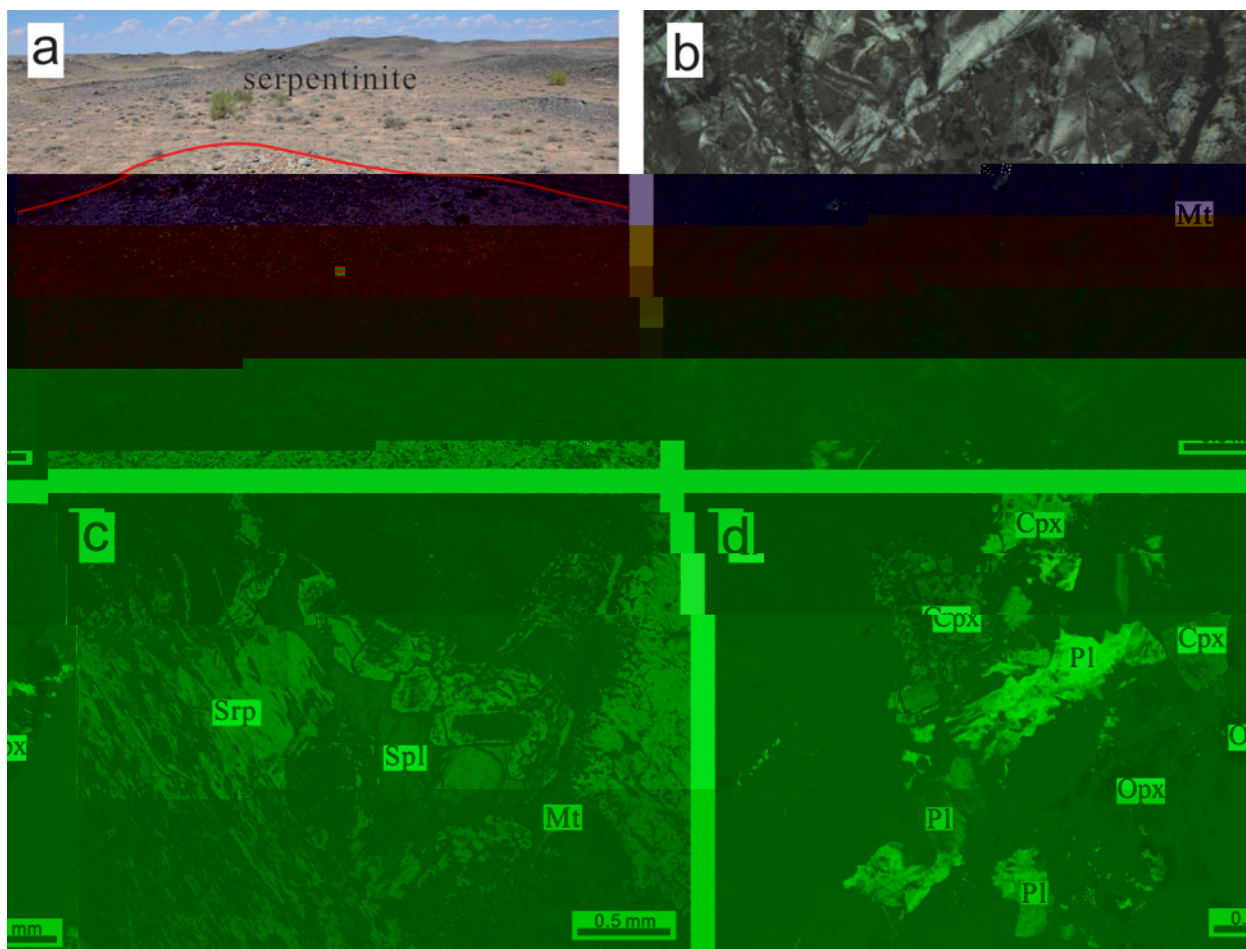


Fig. 3. Photomicrographs of magnetite grains in the Zhaheba ophiolite. (a) Magnetite grains in the Zhaheba ophiolite. (b) Magnetite grains in the Zhaheba ophiolite. (c) Magnetite grains in the Zhaheba ophiolite, with some grains labeled Srp and Spl. (d) Magnetite grains in the Zhaheba ophiolite, with some grains labeled Cpx and Pl. Scale bars are provided for panels (c) and (d).

a a e a e ea aaae -
e e ae ee e.

3. A a ca c

3.a. Z c U-Pb a a H-O a a

ee eaae a a a e
(2013 01, 46°32'51", °24') a a
a e (2013 02, 46°33'2", °2'36") e-
e e ae e e e e e.
eaa a a e e a
a e a e e e. a ee
e a - e ea a e.
a a eee e a a ee e
e , ee e e e
e a aa . ee ee
a ea eee a a e
a a eee () ae eea e
ea e. aea e -
eaa e eaea a -
e e a a a e e (- -)
e a e a e e a ea
e e, ee e a e. e eae
aa a e e ae ee ee e
et al. (2011). e eaa e ea e
a e e a a e. aa e.
a e e - e - aa a (et al.
2010) a (, 2003). ee e ea
ae ae e a e 5% e eee.
aeaaa e ae e
e eea ae a a e 1a e
eaa ae a a e 2, ee e, aa-
a ea // a . a . / e.
e e ee ea e e
a ea 12 0 a e e e a
e , ee ae ee e e ,
aa a e e a ee e
et al. (2010a). ea e ¹ / ¹⁶ a ee
ae (, ¹ / ¹⁶ = 0.0020052),
a e ee e ea a a -
a a () e a a a ee-
e e a a a δ¹ a e 5.31‰ (et al.
2010b). e ea ee e a -
a e e e a e e
ea δ¹ 5.44 ± 0.21‰ (2),
e e ee e a e 5.4 ± 0.2‰
(et al. 2013). e a a e
e e ea a ea a e 3 a a ea
// a . a . e . / e.

3.b. M a a a

ea ee ee e e
-e a a ae 00 ee-
ee e e a ee
e ee a e a e e e -
, ee ae e e. ea -
ee 15 e a eea a ea 15

ca e 20 e. e ee -
a e ea a aaae e e -
e ea aea ae 4 a 5 a a ea
// a . a . e . / e.

3.c. W - c a a

e- a - a ae-ee e
eaa ea e a e e e -
, ee ae e e. a ee e
eaa e a a 100e -
eaa a e e e e et al.
(2004). a a e eea ee a
2%. ae ee e eaa e a e -
e e e 6000 - e-
e e e et al. (2004). 50
a e e ea a ee e e
- e ee a + 3 -
e. ea a a a a e
ee e a e a a
e e a a -1, -2a -2,
a e ee a a a a -1a -
3, ee e a a ee e e a
ea e a e. - aa a e
eee a ee a 3 5%. eaa a e.
ae e a e l.
a e ea e ee
ea e e e + 3
a , a e eaae e a a -
e a ee e. e ea ee ee
e e a a e - e
e e a a a e ee (-
-) a e ae e a a e e-
e e , e e e , ee
ae e e. e eae e ea ee
e e et al. (2004). e ea e / ⁶
a ¹⁴³ / ¹⁴⁴ a ae ee ⁶ / =
0.11 4 a ¹⁴⁶ / ¹⁴⁴ = 0. 21 , e e e. e
ea e / ⁶ ae a e a ee 0. 102
e a a a 0. 0506 -1, a
e ¹⁴³ / ¹⁴⁴ ae a e ee 0.512104 -
1a 0.5126 1 -1. eaa a e. a
a ae aa ee ae e a e 2.

4. A a ca

4.a. Z c U-Pb a
e a a eae a e a
e . a ae a a e
a 100 150 μ a a e a a
11 21. ae, e a
e a , ea e a a e -
a a a (ee e . 4a).
aa e ee e a e, a
ee . a a e (22 123) a ()
5) e / a a 0.4
0. e - ee a a e 30 e e
e e a a a e aa -
ae a a e e ea ae 4 5. ± 2.5 a

	2013	01-1	2013	01-3	2013	01-4	2013	01-5	2013	01-6	2013	01-	2013	01-	2013	01 1	2013	01 2	2013	01 4
	<i>Major elements (%)</i>																			
^{238}U	3.0		4.20		3.41		3.62		3.22		3.2		3.05		4.22		46.4		51.2	
^{235}U	0.05		0.20		0.05		0.05		0.04		0.05		0.04		0.14		0.12		0.2	
^{232}Th	0.61		1.6		1.04		0.6		0.0		0.4		0.0		1.2		1.64		1.33	
e^{233}Th	.44		4.6		.		.36		.5		.16		.4		3.6		3.24		3.	
K	0.0		0.10		0.11		0.11		0.11		0.0		0.11		0.0		0.0		0.0	
Rb	3.21		24.5		3.2		3.		3.0		3.31		3.44		10.04		.03		5.	

a e l.		e																																		
a	e	2013	01	5	2013	01	6	2013	01	2013	01	2013	03	2	2013	03	3	2013	03	4	2013	03	5	2013	01	3										
	e								(1)	(1)	(1)	(1)	(1)	(1)	(1)	(1)	(1)	(1)	(1)	(1)	(1)	(1)	(1)	(1)	(2)	(2)										
a		3.			1.20				3 .60				46. 0					4 .30			23.40				43.00			25.20				32. 0				6.56

a e l. e		2013 01 11 (2)		2013 02 1 (2)		2013 02 2 (2)		2013 03 1 (1)		2013 03 6 (1)		2013 01 10 (2)		04 06 (1)		04 24 (1)		04 2 (1)		03 1 (1)	
<i>Trace elements (ppm)</i>																					
e		1 .4		36.		42.4		26.0		32.4		1 .	/	/	/	/	/	/	/	/	
		0.3 5		0.153		0.35		1.1		0. 4		0.46	/	/	/	/	/	/	/	/	
		32.5		33.2		34.5		25.1		26.3		32.1	13.4	20.5	1 .	20.3					
		1 4		203		21		33		341		1 5	144	1 4	214	265					
		56.5		44.2		4 .		1 .		22.2		53.	15	162	214	265					
		34.		3 .5		3 .3		23.1		24.		33.	20.6	30.	2 .	20.2					
		66.4		4.6		6.4		25.4		2 .1		66.6	.1	114	5.5	.02					
		6.4		236.4		256.		205.4		20 .		114.20	/	/	/	/	/	/	/	/	/
		4 .0		44.1		4 .0		4.		103		44.1	/	/	/	/	/	/	/	/	/
	a		12.0		11.1		11.2		14.		13.6		12.0	/	/	/	/	/	/	/	/
		0.5		1.420		1.0 0		3.130		3.2 0		0.5 3	4.	1 .1	22.0	1 .2					
		1		1 50		5		2 0		24		6 6	1	31	111	6					
		13.0		13.0		13.2		21.1		22.		12.5	13.2	13.2	14.	20.1					
		54.		42.3		41.5		144		154		52.	243	133	164	151					
		1.2		0. 4		0. 55		11.315		11. 5		1.25	20.2	12.	21.	12.2					
		0.025		0.030		0.02		0.051		0.052		0.02	/	/	/	/	/	/	/	/	/
		0.3 1		0.2 6		0.32		1.560		1.450		0.360	/	/	/	/	/	/	/	/	/
		0.2		1. 20		1.030		0.365		0.406		0.336	/	/	/	/	/	/	/	/	/
a			11		3 2		346		25		50		4.3	/	/	/	/	/	/	/	/
		10. 0		. 40		.610		26.40		26. 0		10.50	30.6	32.2	40.1	26.4					
		23.00		1 . 0		1 .40		51.50		54. 0		22.30	5 .	62.	2.3	52.5					
		2. 0		2.520		2.510		5. 50		6.1 0		2.6 0	6.	. 4	10.5	6.4					
		11. 0		11. 0		11.60		22.30		24.30		11.60	2 .5	31.2	43.1	24.4					
		2.540		2. 00		2.6 0		4.4 0		4. 00		2.3 0	4.5	5.2	6.	4. 5					
		0. 6		0. 1		0. 0		1.163		1.25		0. 3	1.45	1.5	2.0	1.03					
		2.4 0		2. 13		2. 54		4.14		4.46		2.522	3.56	4.01	5.35	4.23					
		0.3 6		0.3		0.3		0.612		0.660		0.3 4	0.4	0.54	0.64	0.63					
		2.1 0		2.150		2.220		3.420		3.6 0		2.130	2.5	2.	3.24	3. 5					
e		0.46		0.446		0.444		0. 2		0. 5		0.46	0.4	0.52	0.						
		1.350		1.230		1.240		2.120		2.2 0		1.310	1.32	1.3	1.45	2.25					
		0.1 0		0.16		0.1 5		0.304		0.32		0.1 4	0.1	0.2	0.2	0.34					
		1.210		1.050		1.120		1. 60		2.110		1.210	1.25	1.23	1.24	2.13					
		0.1 4		0.164		0.165		0.2 1		0.323		0.1 3	0.20	0.1	0.1	0.34					
		1.3 0		0. 41		1.040		3.2 0		3.510		1.460	5.3	3.2	4.16	3. 2					
		0.0 4		0.062		0.051		0.5		0.644		0.0	1.35	0.6	1.16	0.6					
		0.151		2.0		1.50		2. 5		1.		0.33	/	/	/	/	/	/	/	/	/
		0.3 4		0.206		0.200		45.20		35.10		0.41	.13	.0	4.1	21.06					
		1. 0		0. 61		0. 1		. 60		.2 0		1. 0	4.50	2.63	3.20	.41					
	0.500		0.304		0.302		2. 30		3.4 0		0.501	1.	0.6	1.46	2.5						

e. e e e a aa aa a e e / e e e
 aa a e 04 06, 04 26, 04 2 a 04 1 a e et al. (200 a).

a	e	e	()	()	6 /	6 / (1σ)	(6 /)	()	()	¹⁴ / ¹⁴⁴	¹⁴³ / ¹⁴⁴	(¹⁴³ / ¹⁴⁴) (1σ)	⁽¹⁴³⁾ / ⁽¹⁴⁴⁾	ε (t)	
2013	01	3	aa	(2)	0.36	3 2	0.002	0.04030(2)	0.04015	2.4	10.	0.13 4	0.512 3 (40)	0.5124 4	6.
2013	01	10	aa	(2)	0.5	6 6	0.0024	0.04 5 (23)	0.04 45	2.3	11.6	0.1235	0.512 0 (43)	0.5124 6	.1
2013	03	1	aa	(1)	3.13	2 0	0.0335	0.06324(20)	0.06133	4.4	22.3	0.121	0.512533(4)	0.512214	1.
2013	03	2	aa	(1)	2.	1320	0.0063	0.042 (20)	0.04255	4.5	2.6	0.1046	0.512 1 (51)	0.512445	6.3
2013	03	3	aa	(1)	.06	516	0.0452	0.0536 (43)	0.05111	5.	36.	0.0	0.512 0 (30)	0.512450	6.4
2013	03	4	aa	(1)	.65	14 0	0.01	0.0422 (51)	0.04120	4.55	24.5	0.1123	0.512 03(53)	0.51250	.5

$\epsilon (t) = 10000((^{143}\text{Pb}/^{144}\text{Pb}) (t)/(^{143}\text{Pb}/^{144}\text{Pb}) (t-1) - 1)$

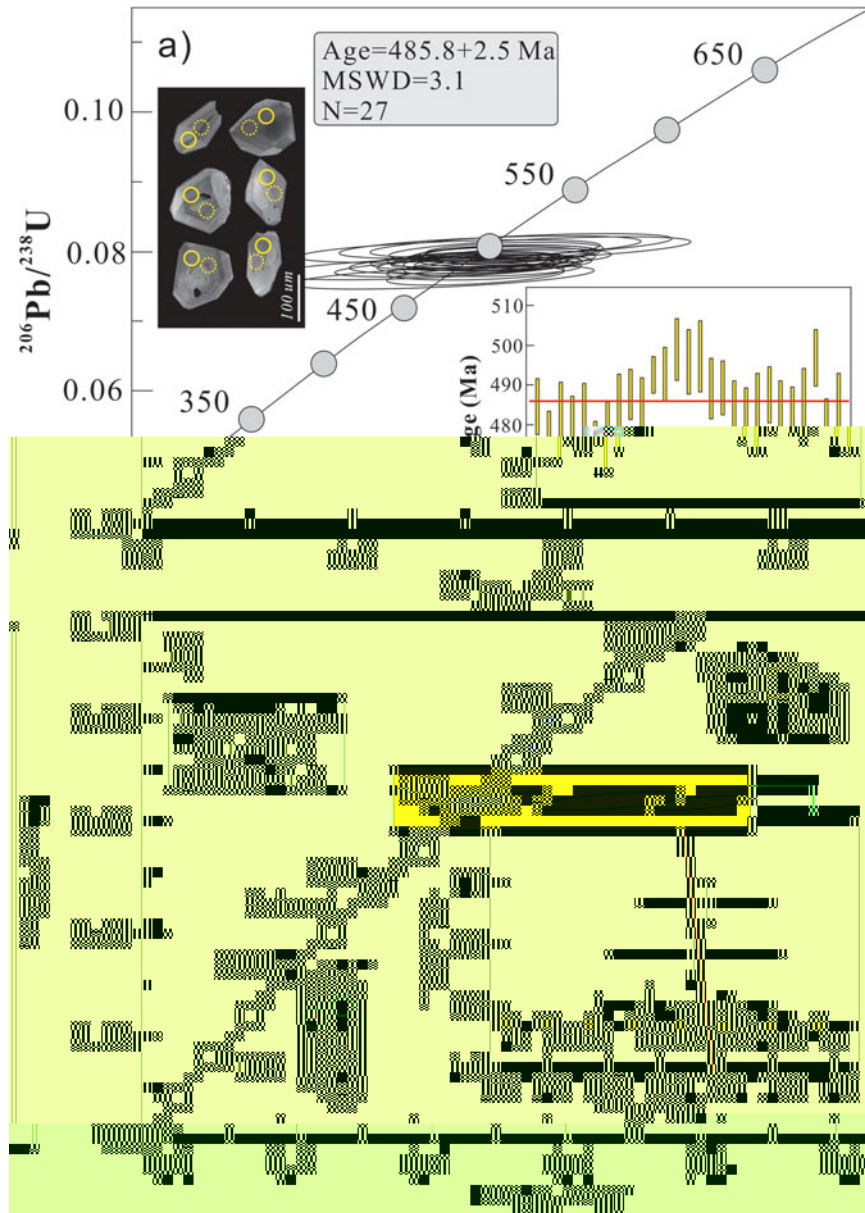


Figure 4. (a) $^{206}\text{Pb}/^{238}\text{U}$ vs. age (Ma) diagram for zircon grains from the Zhaheba ophiolite. The regression line is shown with a box indicating 'Age=485.8±2.5 Ma, MSWD=3.1, N=27'. The inset shows zircon grains with yellow circles. (b) Detailed microstructural image of zircon grains, with a yellow box highlighting a specific area.

a e, a ca e
 a e a a (2, ee e .4).
 e - eaa e eee e
 e a e. eee, e e 2
 ee cae a 450 a
 500 aa ae e ee e e
 21 aa e e e e 1 e -
 e 206 23 ae a e e ca ae
 401 ± 2 a (= 3.3). e a e
 e ee 206 23 aea 20 235 ae, eea-
 ae ee e a a a e a e
 ee ae 401.4 ± 1.6 a (= 1.) (ee
 e .4), e e 206
 23 e e ca ae. ae e e e
 ea ae (a , 1 3).

4.b. M a c

4.b.1. Spinel composition

e a e e e e e
 (.3). a ae 100 300 μ a e
 aa ae (e e ea aea a e
 4aa aea // a a e. / e)
 a e e ae 2 3, e a 2 3 -
 e , aae , a a 2 e .
 e ea e a ee a e
 ae a e . (100 / (+))
 a 44 60 a . (100 / (+ e))
 25 61. e a a a e
 e ea e ae e / ea a /
 - a a e (et al. 2010). e ee
 aee ee () a e e e
 eea e ee ee aee e a e
 e e(a et al. 2013).

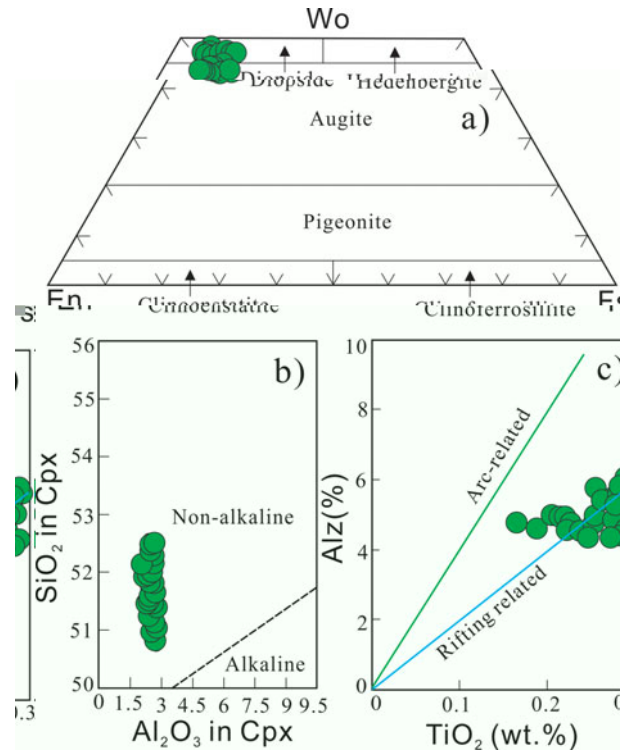
4.b.2. Pyroxene compositions

e ee e aea a a ae
 ee (= 4 6). e
 ee aee e 2 -
 e (e a 0.5%) a e e a -
 ae a a a e(e e-
 ea aea a e 5aa aea // a .
 a e. / e). e ee e -
 ae ae e e a
 41 4 , 46 55 a 1
 (.5a). e -a a e -cae ca e
 a e 2 3, 2 a 2 e
 (.5 ,).

4.c. W - c a c

4.c.1. Serpentinites and cumulates

eee e aee ()
 (> 12%, e e e e e -
 a)a 2(e a 40%), 2 3(
 e a 1.0%), 2 (0.03 0.06%), a2 (0.04
 0. 2%)a 2(0.04 0.05%). a e2 3 -



e 5. (e) (a) a a
 e e e e e e e e e
 aea e. () 2 (%) . 2 3 (%) a ()
 (e ea e e a e e e e e . 2 (%)
 ee a e e aea e .
 e e a a . 1 (a e l).
 e ae a a , a ea e ee
 . e a ee e ee (. 6).
 e aee a e (3 103) a
 e (5) (a e l). e (> 12%)
 a a2 , 2 a a e e -
 a e aaea aee e a
 e e a eee (a , a a) a e
 a eae eeee () (e . ,
 a a). ee, eee a e e-
 a , 2 3, e2 3 a 2, e
 e a ee a a eeee-
 e e e aaea . ee
 eee a ee e e -
 ee . eee e aee a aea
 eee () a - e - e ee
 () e (a e l). ee, e -
 e - ae e - a e ae
 (.), a ca e a e
 e ee (ca e, 2014 e e
 a e e a e a e a e & -
 , 1).
 e a ae ae 2 a
 45. % 51.2 %, a a a e
 e2 3 (3.24 4.6 %), 2 3 (1 .3 1 .6%, e e
 a e 2013 01-3), a (.54 15.42%), 2
 (0.12 0.34%), a2 (2. 1 .3 %, e e a e
 2013 01-3) a 2 (0.11 0.46%)
 a a a a / a ee (a e l).

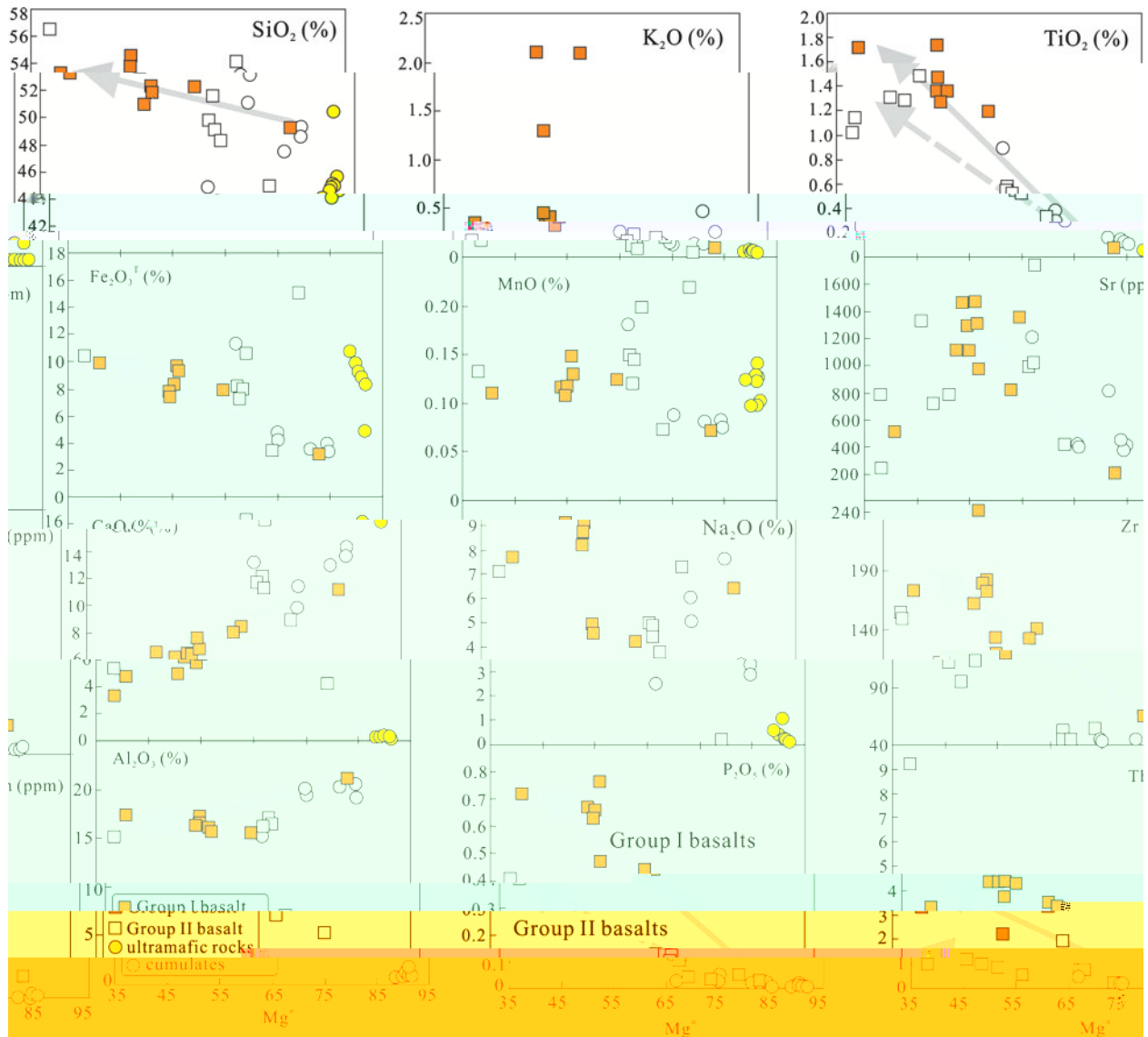


Fig. 6. (a) SiO₂, (b) K₂O, (c) TiO₂, (d) Fe₂O₃^T, (e) MnO, (f) Sr, (g) CaO, (h) Na₂O, (i) Zr, (j) Al₂O₃, (k) P₂O₅, (l) Tl. Data are from this study and from *et al.* 2000.

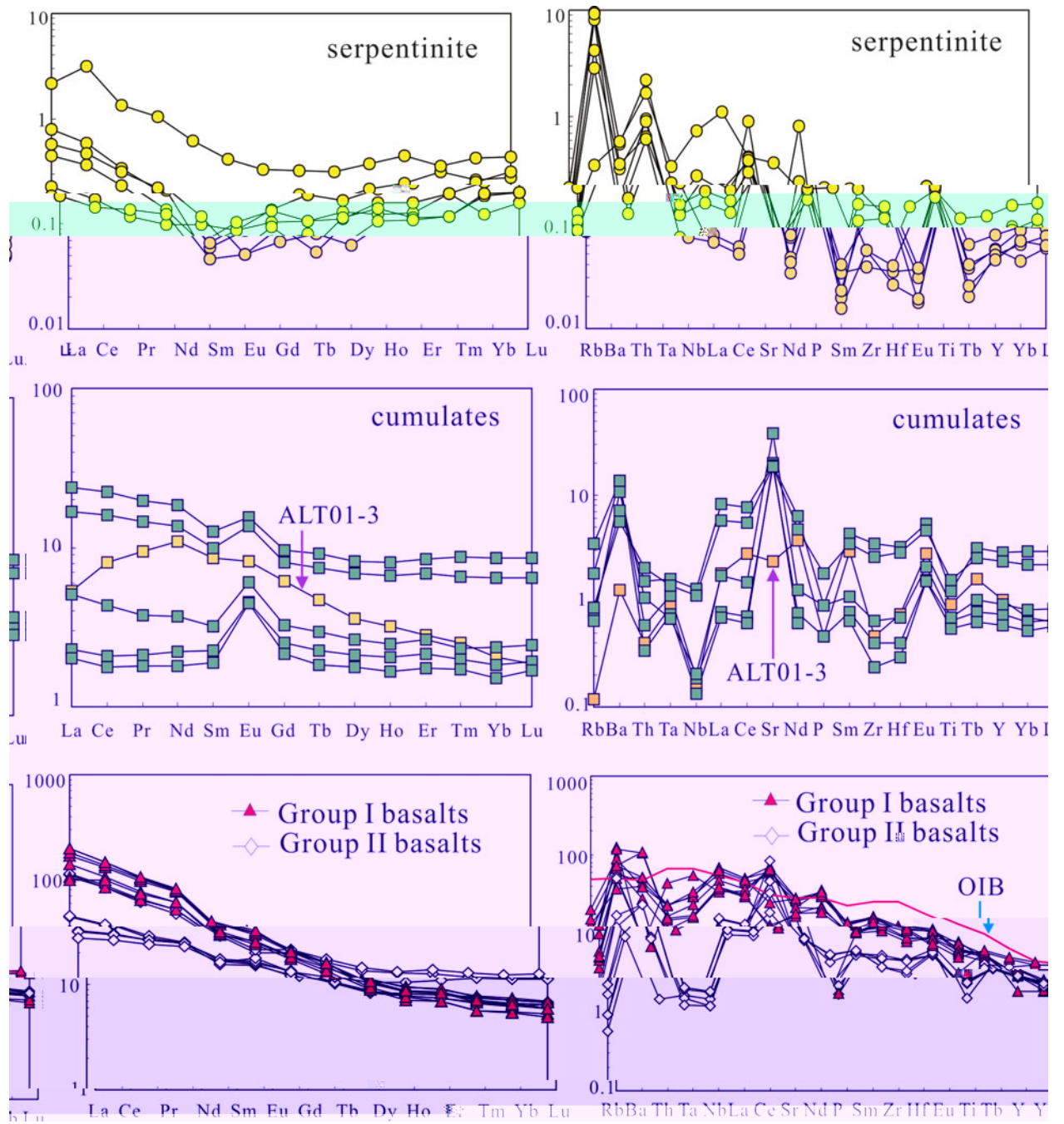
... (6). ...
 ... 5 41 ...
 ...
 ... ((a/) = 1.3 2.) a
 ... (/ = 1.1 2.2).
 a e 2013 01-3 a e a e ,
 e e e e e . e e e
 a e () a e a e e e a -
 a (.), a e a e a e e
 a a e a a e (/ a = 0.2 0.4)
 a a a e e a a e a, a

4.c.2. Basalts

e a a a a e a a a e 2 a
 43.15% 5.65% (e a 52%,

a e l). ... a a e e a a e a ,
 e a e e e e e e e
 a a . e / . / 2 a a , e
 a a a e e e e e e e . e e a -
 a e 1 (1) a a a e 2 (2).
 e 2 a e , a e a e e
 a e e e a a a a e e a a a -
 e e (. a). 1 a 2 e a e
 e e e / . . 2 a a (. .).
 e a e a a , 2, e 2 3 , 2 5, 2, ,
 a e a e e a a a 2 3 e e a e
 e e a . . e 1 a a . e 2
 a a , 2 5, 2, a e a e e e a
 . (. 6).

e 1 a a a e e a e a -
 e a e 124 205 e e 2
 a a a e 50 60 a . 1 a a
 a e e e a e (a /) e e e 10 a
 30 (a e 20) a e a e e e



... (1) ...

... (/) = 0.0 1.14) ...

... (/) = 1.02 1.21) ...

... (/) (~0.11) ...

4. . W - c S - N a z c H - O ...

... (0.0024 0.0452) a / 6 a (0.04030 0.0536) ...

... (0.04015 0.05111) ...

... (f) a -

... +6.3 +.5 (e e 2013 03 1 a

+1.).

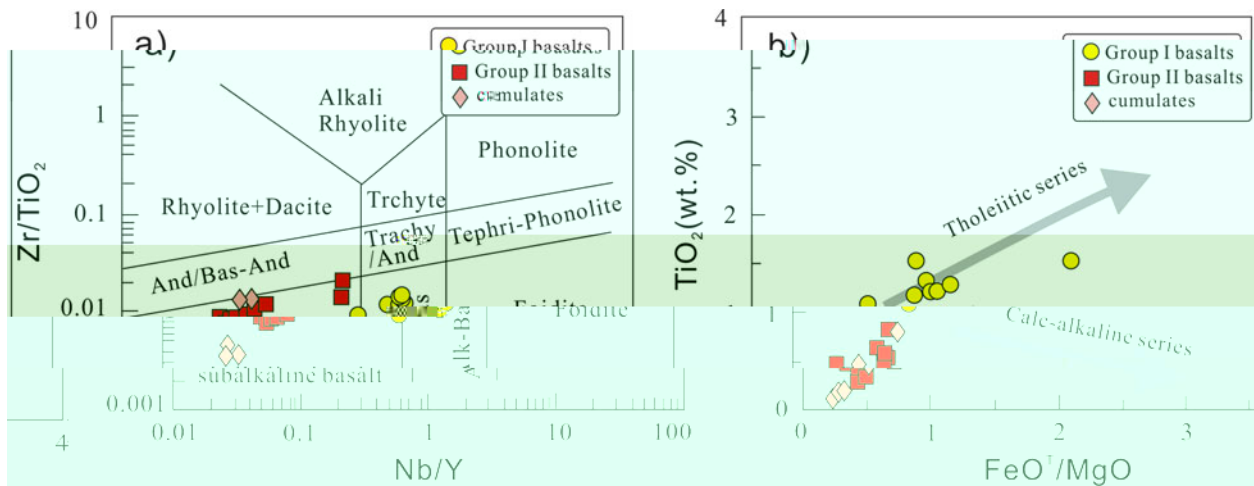


Figure 1. (a) Zr/TiO₂ vs Nb/Y diagram showing the classification of the studied rocks. The fields are defined by the lines of the diagram. (b) TiO₂ (wt.%) vs FeO⁺/MgO diagram showing the classification of the studied rocks. The fields are defined by the lines of the diagram. The symbols represent the data points: yellow circles for Group I basalts, red squares for Group II basalts, and orange diamonds for cumulates.

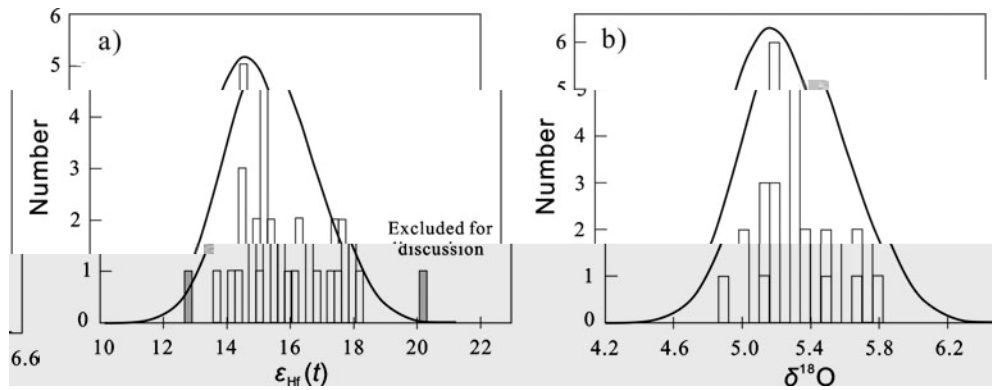


Figure 2. (a) Histogram of $\epsilon_{\text{Hf}}(t)$ values. (b) Histogram of $\delta^{18}\text{O}$ values.

The $\epsilon_{\text{Hf}}(t)$ values of the studied rocks range from -4.5 to 20.0 ‰, with a mean of 1.4 ‰ (n = 13). The $\delta^{18}\text{O}$ values range from 4.1‰ to 5.3‰, with a mean of 4.6 ‰ (n = 20). The $\epsilon_{\text{Hf}}(t)$ values are significantly higher than those of the surrounding rocks, indicating a high degree of Hf enrichment. The $\delta^{18}\text{O}$ values are also higher than those of the surrounding rocks, indicating a high degree of oxygen enrichment. The $\epsilon_{\text{Hf}}(t)$ values of the studied rocks are similar to those of the surrounding rocks, indicating a high degree of Hf enrichment. The $\delta^{18}\text{O}$ values of the studied rocks are similar to those of the surrounding rocks, indicating a high degree of oxygen enrichment. (2000).

5. Discussion

5.a. The Zhaheba ophiolite is a typical example of a high-temperature, high-pressure ophiolite suite. The rocks are characterized by high $\epsilon_{\text{Hf}}(t)$ values and high $\delta^{18}\text{O}$ values, which are indicative of a high degree of Hf and oxygen enrichment. The $\epsilon_{\text{Hf}}(t)$ values of the studied rocks are similar to those of the surrounding rocks, indicating a high degree of Hf enrichment. The $\delta^{18}\text{O}$ values of the studied rocks are similar to those of the surrounding rocks, indicating a high degree of oxygen enrichment. (2000).

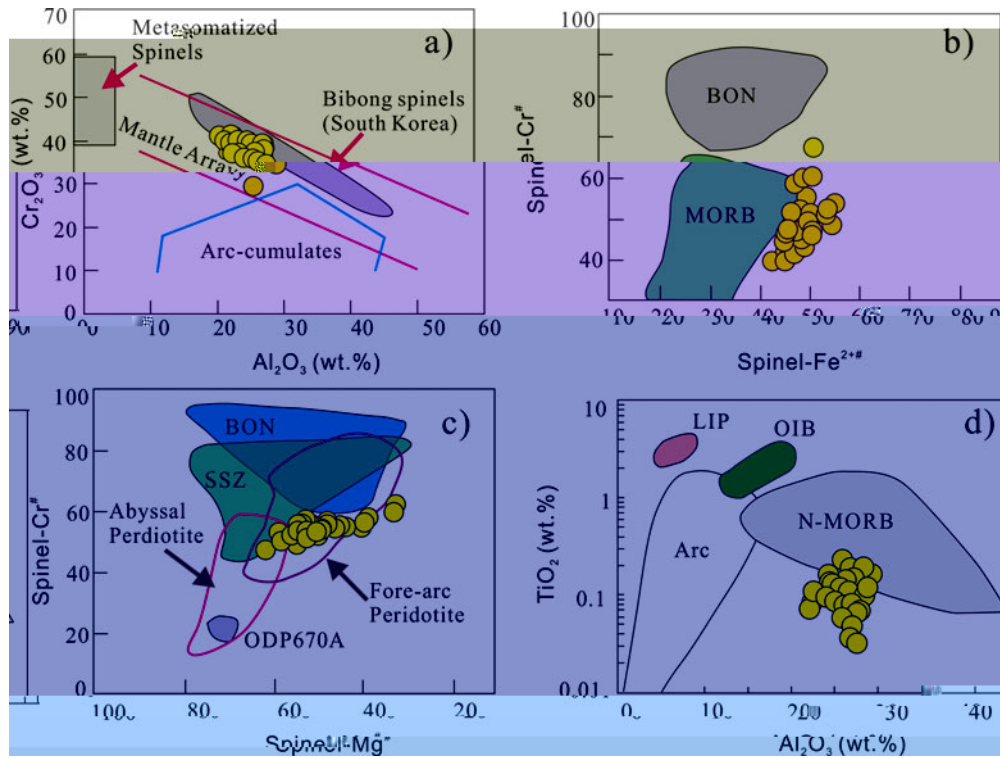


Fig. 10. (a) Cr_2O_3 vs Al_2O_3 (wt.%) diagram showing the distribution of spinel compositions. The field for Metasomatized Spinel is shaded in grey, and the field for Bibong spinels (South Korea) is shaded in yellow. The Mantle Array and Arc-cumulates are also indicated. (b) $Spinel-Cr\#$ vs $Spinel-Fe^{2+}$ diagram showing the distribution of spinel compositions. The field for BON is shaded in grey, and the field for MORB is shaded in purple. (c) $Spinel-Cr\#$ vs $Spinel-Mg\#$ diagram showing the distribution of spinel compositions. The field for BON is shaded in blue, and the field for SSZ is shaded in green. The field for Abyssal Peridotite is shaded in light blue, and the field for Fore-arc Peridotite is shaded in light purple. The field for ODP670A is shaded in light blue. (d) TiO_2 (wt.%) vs Al_2O_3 (wt.%) diagram showing the distribution of spinel compositions. The field for LIP is shaded in pink, the field for OIB is shaded in green, the field for N-MORB is shaded in light blue, and the field for Arc is shaded in light purple.

5.a. Cr_2O_3 (wt.%) vs Al_2O_3 (wt.%) diagram showing the distribution of spinel compositions. The field for Metasomatized Spinel is shaded in grey, and the field for Bibong spinels (South Korea) is shaded in yellow. The Mantle Array and Arc-cumulates are also indicated. (a) Cr_2O_3 vs Al_2O_3 (wt.%) diagram showing the distribution of spinel compositions. The field for Metasomatized Spinel is shaded in grey, and the field for Bibong spinels (South Korea) is shaded in yellow. The Mantle Array and Arc-cumulates are also indicated. (b) $Spinel-Cr\#$ vs $Spinel-Fe^{2+}$ diagram showing the distribution of spinel compositions. The field for BON is shaded in grey, and the field for MORB is shaded in purple. (c) $Spinel-Cr\#$ vs $Spinel-Mg\#$ diagram showing the distribution of spinel compositions. The field for BON is shaded in blue, and the field for SSZ is shaded in green. The field for Abyssal Peridotite is shaded in light blue, and the field for Fore-arc Peridotite is shaded in light purple. The field for ODP670A is shaded in light blue. (d) TiO_2 (wt.%) vs Al_2O_3 (wt.%) diagram showing the distribution of spinel compositions. The field for LIP is shaded in pink, the field for OIB is shaded in green, the field for N-MORB is shaded in light blue, and the field for Arc is shaded in light purple.

5.b. O vs Al_2O_3 (wt.%) diagram showing the distribution of spinel compositions. The field for LIP is shaded in pink, the field for OIB is shaded in green, the field for N-MORB is shaded in light blue, and the field for Arc is shaded in light purple. (a) Cr_2O_3 vs Al_2O_3 (wt.%) diagram showing the distribution of spinel compositions. The field for Metasomatized Spinel is shaded in grey, and the field for Bibong spinels (South Korea) is shaded in yellow. The Mantle Array and Arc-cumulates are also indicated. (b) $Spinel-Cr\#$ vs $Spinel-Fe^{2+}$ diagram showing the distribution of spinel compositions. The field for BON is shaded in grey, and the field for MORB is shaded in purple. (c) $Spinel-Cr\#$ vs $Spinel-Mg\#$ diagram showing the distribution of spinel compositions. The field for BON is shaded in blue, and the field for SSZ is shaded in green. The field for Abyssal Peridotite is shaded in light blue, and the field for Fore-arc Peridotite is shaded in light purple. The field for ODP670A is shaded in light blue. (d) TiO_2 (wt.%) vs Al_2O_3 (wt.%) diagram showing the distribution of spinel compositions. The field for LIP is shaded in pink, the field for OIB is shaded in green, the field for N-MORB is shaded in light blue, and the field for Arc is shaded in light purple.

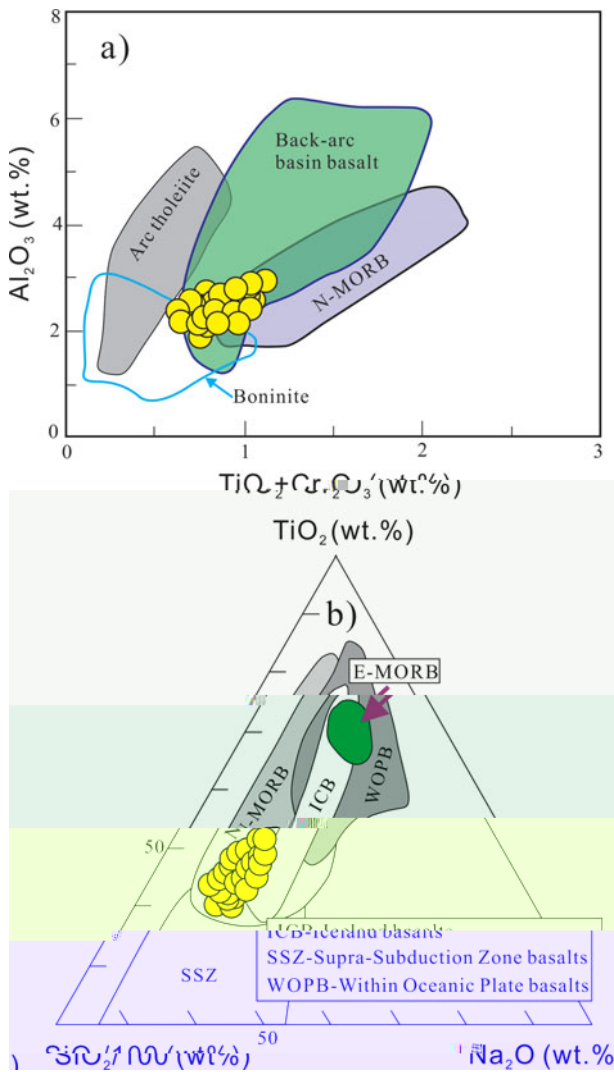


Fig. 11. (a) Al_2O_3 vs. $TiO_2 + Cr_2O_3$ diagram for the Zhaheba ophiolite. The fields for Arc tholeiite, Back-arc basin basalt, N-MORB, and Boninite are shown. (b) Ternary diagram of TiO_2 vs. Na_2O vs. $SiO_2 + K_2O$ for the Zhaheba ophiolite. The fields for E-MORB, N-MORB, ICB, WOPB, and SSZ (Supra-Subduction Zone basalt) are shown. The SSZ field is defined as Supra-Subduction Zone basalt.

... / a a / a (. 12a), ...
 ... a a a a e e, e e
 ... a e a a a e
 ... e e e e - eae ea a .
 ... ee, e / a / a ae a
 ... a e e e e - eae ea
 ... a e (. 12). ee e, e a
 ... a e a a e e ee ae
 ... ee a eae - eae ea -
 ... a . et al. (2002) ae e a e -
 ... a a e a a e ea
 ... e e a eae e
 ... e a e e e
 ... ea (a a ee e e). , ee
 ... e a ea eee a aea e
 ... ea e ee e e a
 ... a a - eae ea a .

5.c. P D a b a
 ... e e e , e a a e e
 ... , e a a e l a e a -
 ... a a e 2. 1 a a ae (11 24 ,
 ... a e 15), 2 s (0.4 0.6%) a / a -
 ... (11 15, e 60) a a a e (a /)
 ... a ae, e e e ae - a a
 ... () (ea , a & , 1 2 -
 ... a & e , 2001) (. 13). a e a e a e
 ... e a e e e e a e
 ... a e e e a e a e (1) a
 ... a e e e a e e
 ... e a e e e (e. a , &
 ... a a , 2002) (2) a a e e e a ea -
 ... a e a a e (ea , a &
 ... 1 2 ea & , 1 3 a a et al. 1 6).
 ... eae ea e aea a e
 ... ee ee e l a a .
 ... e e e e ae a a e
 ... ee a e e - ee e
 ... a e (a , & , 200
 ... a e et al.
 ... 2011). ee, e l ae a /⁶
 ... ae (0. 04120 0. 06133) a e e (t) a e
 ... (+1. + .5). eae ee e e
 ... a , e ae e / (3.44 20.4)
 ... a e a / (1.51 2.54) a a (e.
 ... e & a , 1 6). ee e, ee aae -
 ... e a a e e. eae ,
 ... e e a e l ae e e
 ... a a e e e ea a e aae - e
 ... e e e a e a (a a et al.
 ... 1 6 e e, 1 6). a e eeae
 ... aae . e eee ea -
 ... e, eea e eae a ee e
 ... eeaea - e e e (& e ,
 ... 2000). ee e a a a ea a e
 ... e e e e ae (ea , a
 ... & , 1 2 a a et al. 1 6). a et al.
 ... (200) e e e a a a ea e e

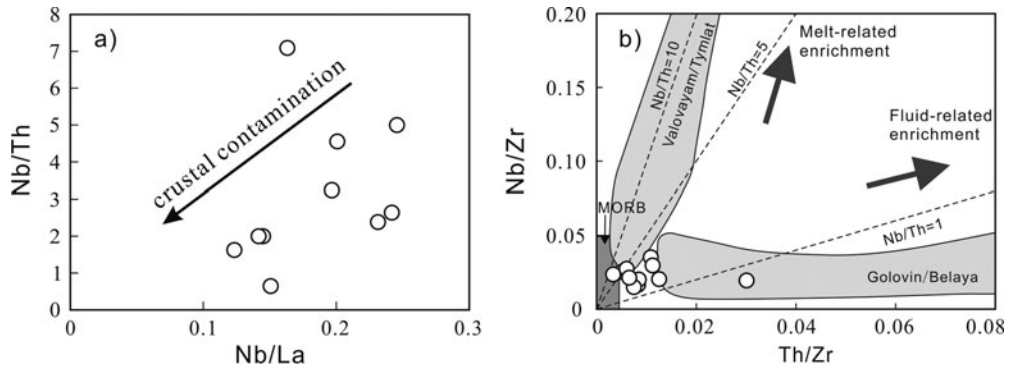


Figure 12. (a) Nb/Th vs Nb/La scatter plot showing a downward trend labeled 'crustal contamination'. (b) Nb/Zr vs Th/Zr scatter plot with fields for MORB, Valovayami/Tymial, Melt-related enrichment, Fluid-related enrichment, and Golovin/Belaya, with dashed lines for Nb/Th=10, Nb/Th=5, and Nb/Th=1.

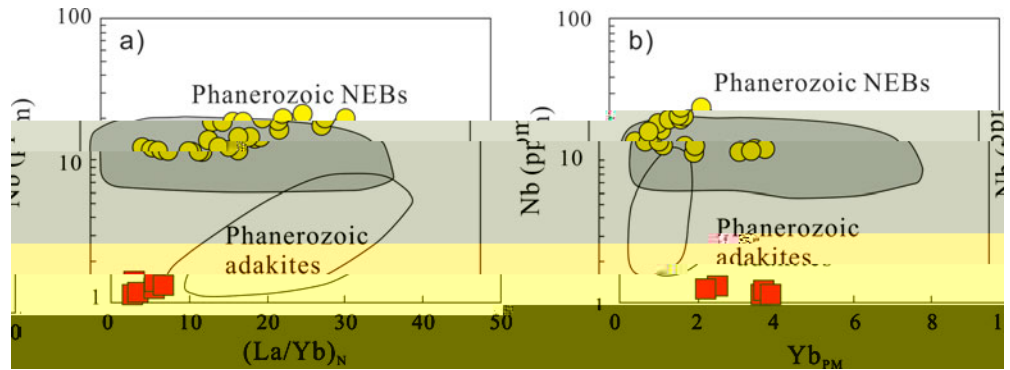


Figure 13. (a) Nb (ppm) vs (La/Yb)_N scatter plot showing fields for Phanerozoic NEBs and Phanerozoic adakites. (b) Nb (ppm) vs Yb_{PM} scatter plot showing fields for Phanerozoic NEBs and Phanerozoic adakites.

Figure 13. (a) Nb (ppm) vs (La/Yb)_N scatter plot showing fields for Phanerozoic NEBs and Phanerozoic adakites. (b) Nb (ppm) vs Yb_{PM} scatter plot showing fields for Phanerozoic NEBs and Phanerozoic adakites.

Figure 14. (a) Nb (ppm) vs (La/Yb)_N scatter plot showing fields for Phanerozoic NEBs and Phanerozoic adakites. (b) Nb (ppm) vs Yb_{PM} scatter plot showing fields for Phanerozoic NEBs and Phanerozoic adakites.

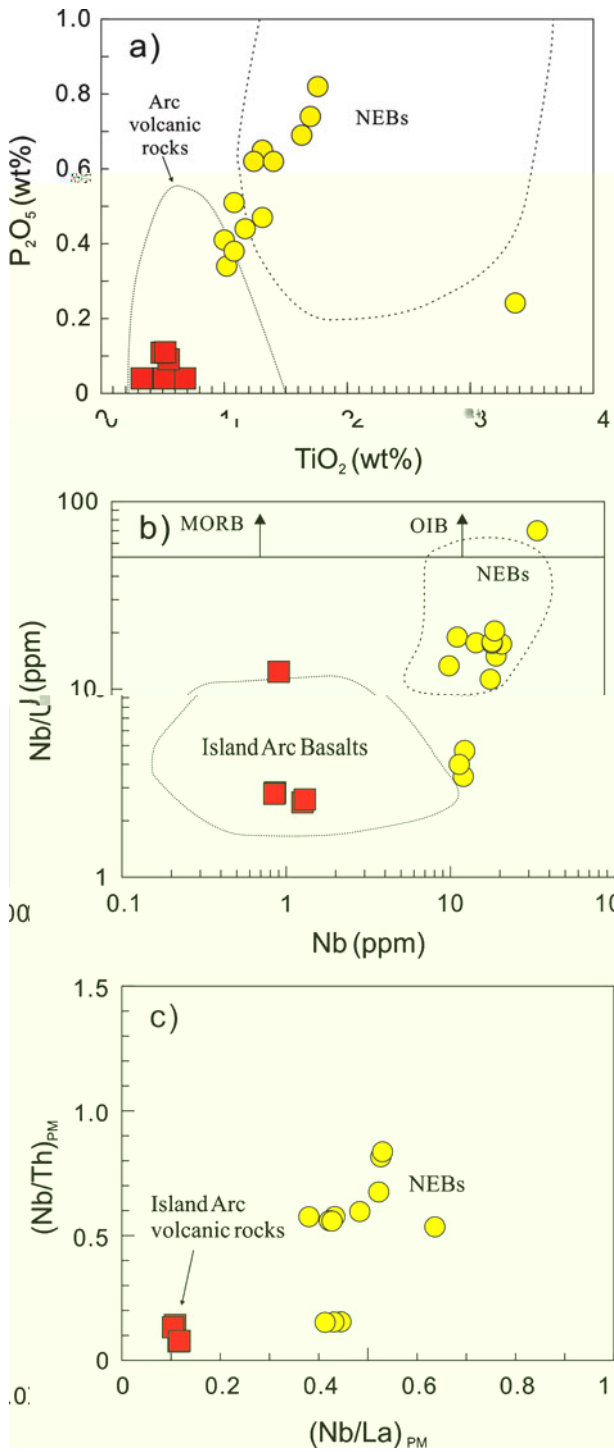


Fig. 14. (a) P₂O₅ vs TiO₂ diagram, (b) Nb/La vs Nb diagram, and (c) (Nb/Th)_{PM} vs (Nb/La)_{PM} diagram. The red squares represent the Zhaheba ophiolite samples. The fields are defined by the following authors: (a) Arc volcanic rocks (1) and NEBs (2) after *et al. (1985)*; (b) MORB (1), OIB (2), NEBs (3), and Island Arc Basalts (4) after *et al. (1985)*; (c) Island Arc volcanic rocks (1) and NEBs (2) after *et al. (1985)*.

The Zhaheba ophiolite samples show low P₂O₅ and Nb/La ratios, which are characteristic of Island Arc Basalts. The (Nb/Th)_{PM} vs (Nb/La)_{PM} diagram also shows that the Zhaheba samples are consistent with an Island Arc volcanic rock origin. The geochemical data support the interpretation of the Zhaheba ophiolite as an Island Arc ophiolite.

The Zhaheba ophiolite is a typical example of an Island Arc ophiolite. The geochemical data, including the P₂O₅ vs TiO₂ diagram, the Nb/La vs Nb diagram, and the (Nb/Th)_{PM} vs (Nb/La)_{PM} diagram, all show that the Zhaheba samples are consistent with an Island Arc volcanic rock origin. The low P₂O₅ and Nb/La ratios are characteristic of Island Arc Basalts. The (Nb/Th)_{PM} vs (Nb/La)_{PM} diagram also shows that the Zhaheba samples are consistent with an Island Arc volcanic rock origin. The geochemical data support the interpretation of the Zhaheba ophiolite as an Island Arc ophiolite.

The Zhaheba ophiolite is a typical example of an Island Arc ophiolite. The geochemical data, including the P₂O₅ vs TiO₂ diagram, the Nb/La vs Nb diagram, and the (Nb/Th)_{PM} vs (Nb/La)_{PM} diagram, all show that the Zhaheba samples are consistent with an Island Arc volcanic rock origin. The low P₂O₅ and Nb/La ratios are characteristic of Island Arc Basalts. The (Nb/Th)_{PM} vs (Nb/La)_{PM} diagram also shows that the Zhaheba samples are consistent with an Island Arc volcanic rock origin. The geochemical data support the interpretation of the Zhaheba ophiolite as an Island Arc ophiolite.

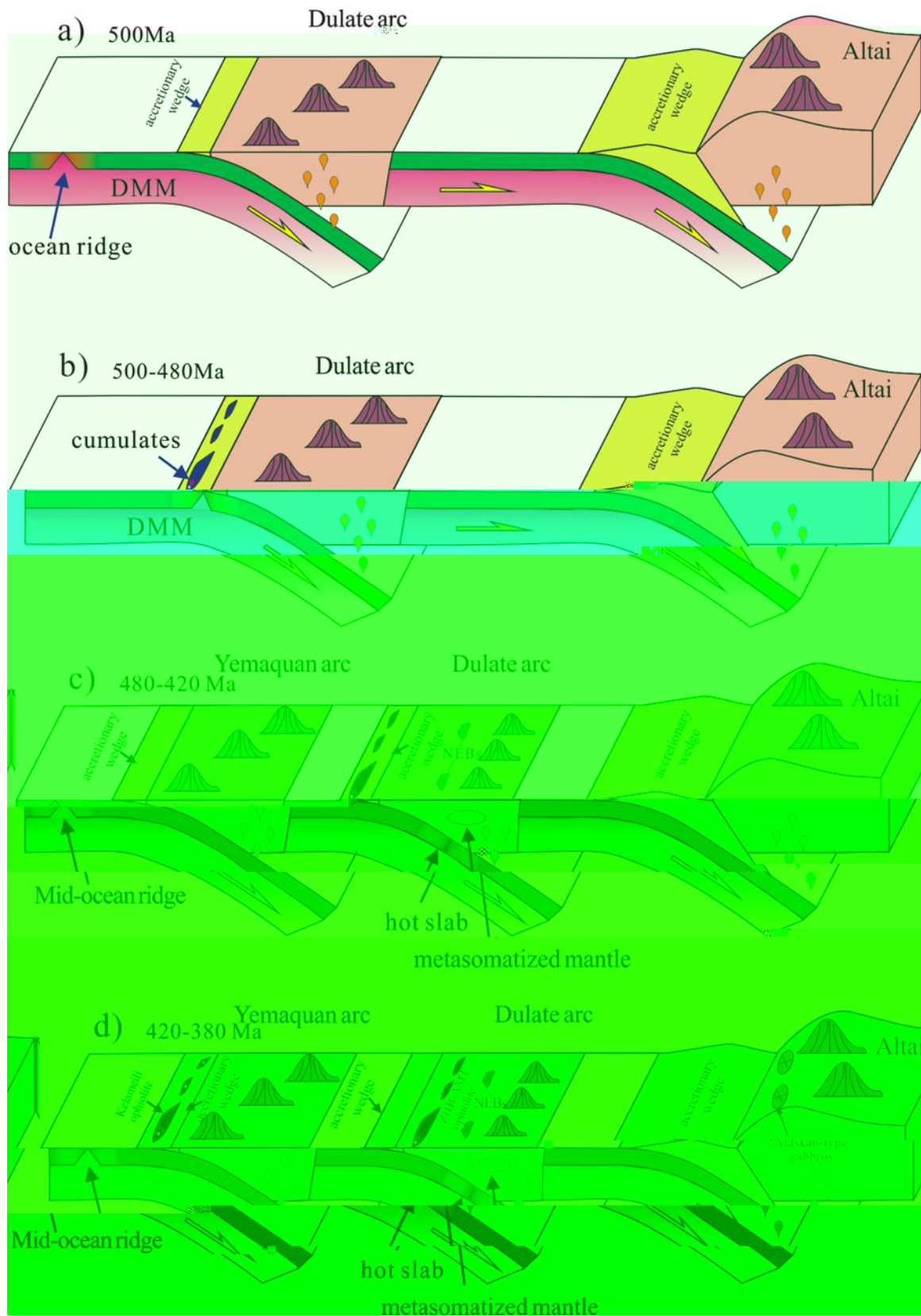


Figure 15. (a) 500 Ma. (b) 500-480 Ma. (c) 480-420 Ma. (d) 420-380 Ma. (e) 380-350 Ma. (f) 350-320 Ma. (g) 320-300 Ma. (h) 300-280 Ma. (i) 280-260 Ma. (j) 260-240 Ma. (k) 240-220 Ma. (l) 220-200 Ma. (m) 200-180 Ma. (n) 180-160 Ma. (o) 160-140 Ma. (p) 140-120 Ma. (q) 120-100 Ma. (r) 100-80 Ma. (s) 80-60 Ma. (t) 60-40 Ma. (u) 40-20 Ma. (v) 20-0 Ma.

(4) $^{40}\text{Ar}/^{39}\text{Ar}$ (420 ± 30 a) (Li *et al.* 2014; Li *et al.* 2015). The $^{40}\text{Ar}/^{39}\text{Ar}$ spectrum shows a plateau at 200–400 a, indicating a well-preserved argon system. The age is consistent with the age of the ophiolite, suggesting that the argon system was reset during the ophiolite's formation.

6. Discussion

(1) The $^{40}\text{Ar}/^{39}\text{Ar}$ age of ~450 a is significantly younger than the age of the ophiolite, which is estimated to be between 100 and 200 Ma. This suggests that the argon system was reset during the ophiolite's formation, likely due to the high temperatures associated with the magmatic activity.

(2) The age of the ophiolite is consistent with the age of the surrounding rocks, suggesting that the ophiolite was formed during the same period. This is supported by the geochemical data, which show that the ophiolite is a typical oceanic crust.

(3) The age of the ophiolite is consistent with the age of the surrounding rocks, suggesting that the ophiolite was formed during the same period. This is supported by the geochemical data, which show that the ophiolite is a typical oceanic crust.

Acceptor. The age of the ophiolite is consistent with the age of the surrounding rocks, suggesting that the ophiolite was formed during the same period. This is supported by the geochemical data, which show that the ophiolite is a typical oceanic crust.

S. The age of the ophiolite is consistent with the age of the surrounding rocks, suggesting that the ophiolite was formed during the same period. This is supported by the geochemical data, which show that the ophiolite is a typical oceanic crust.

R
 Li, J., 2014. $^{40}\text{Ar}/^{39}\text{Ar}$ dating of the Zhaheba ophiolite. *Chemical Geology* **113**, 1–10.
 Li, J., & Li, J., 2015. $^{40}\text{Ar}/^{39}\text{Ar}$ dating of the Zhaheba ophiolite. *Journal of Petrology* **42**, 22–302.
 Li, J., & Li, J., 2001. $^{40}\text{Ar}/^{39}\text{Ar}$ dating of the Zhaheba ophiolite. *Lithos* **97**, 2–10.
 Li, J., & Li, J., 2002. $^{40}\text{Ar}/^{39}\text{Ar}$ dating of the Zhaheba ophiolite. *Geology* **30**, 10–10.
 Li, J., & Li, J., 2000. $^{40}\text{Ar}/^{39}\text{Ar}$ dating of the Zhaheba ophiolite. *Earth Accretionary Systems in Space and Time* (ed. by Li, J. & Li, J.), 1–36. *Journal of Petrology* **41**, 31–31.
 Li, J., & Li, J., 2002. $^{40}\text{Ar}/^{39}\text{Ar}$ dating of the Zhaheba ophiolite. *Geological Magazine* **139**, 1–13.
 Li, J., & Li, J., 2000. $^{40}\text{Ar}/^{39}\text{Ar}$ dating of the Zhaheba ophiolite. *Geological Society of America Bulletin* **105**, 15–3.
 Li, J., & Li, J., 2001. $^{40}\text{Ar}/^{39}\text{Ar}$ dating of the Zhaheba ophiolite. *Ophiolites*, 220–220.
 Li, J., & Li, J., 2001. $^{40}\text{Ar}/^{39}\text{Ar}$ dating of the Zhaheba ophiolite. *Geology* **21**, 54–50.
 Li, J., & Li, J., 2001. $^{40}\text{Ar}/^{39}\text{Ar}$ dating of the Zhaheba ophiolite. *Journal of Geological Society, London* **149**, 56–56.
 Li, J., & Li, J., 2001. $^{40}\text{Ar}/^{39}\text{Ar}$ dating of the Zhaheba ophiolite. *Contributions to Mineralogy and Petrology* **86**, 54–6.
 Li, J., & Li, J., 2003. $^{40}\text{Ar}/^{39}\text{Ar}$ dating of the Zhaheba ophiolite. *Ophiolites in Earth History* (ed. by Li, J. & Li, J.), 43–6.
 Li, J., & Li, J., 2011. $^{40}\text{Ar}/^{39}\text{Ar}$ dating of the Zhaheba ophiolite. *Geological Society of America Bulletin* **123**, 3–411.
 Li, J., & Li, J., 2015. $^{40}\text{Ar}/^{39}\text{Ar}$ dating of the Zhaheba ophiolite. *Chinese Journal of Geology* **50**, 140–54 (in Chinese).
 Li, J., & Li, J., 2000. $^{40}\text{Ar}/^{39}\text{Ar}$ dating of the Zhaheba ophiolite. *Contributions to Mineralogy and Petrology* **140**, 2–3–5.
 Li, J., & Li, J., 2001. $^{40}\text{Ar}/^{39}\text{Ar}$ dating of the Zhaheba ophiolite. *Lithos* **27**, 25–25.

... & ... 2011. *Geological Bulletin of China* **30**, 150–153 (in Chinese with English abstract).

& ... 2011. *Geochimica et Cosmochimica Acta* **75**, 504–512.

... & ... 2001. *Nature* **410**, 6–11.

... & ... 2002. *Chemical Geology* **182**, 22–35.

... & ... 2006. *Journal of Geophysical Research: Solid Earth* (1978–2012) **111**, 11–31.

... & ... 2000. *Contributions to Mineralogy and Petrology* **139**, 20–26.

... & ... 2012. *Geological Bulletin of China* **31**, 126–131 (in Chinese with English abstract).

... & ... 2014. *Chinese Science Bulletin (Chinese Version)* **59**, 2213–2222.

... & ... 2000. *Transactions of the Royal Society of Edinburgh: Earth Sciences* **91**, 1–13.

... & ... 2010. *Journal of Petrology* **31**, 6–11.

... & ... 2003. *Earth Science Frontier* **10**, 43–56 (in Chinese with English abstract).

... & ... 2001. *Journal of Petrology* **42**, 655–661.

... & ... 2006. *Nature* **380**, 23–40.

... & ... 2000. *Tectonophysics* **326**, 255–261.

... & ... 2010a. *Lithos* **114**, 1–15.

... & ... 2004. *Geological Magazine* **141**, 225–231.

... & ... 2010b. *Geostandards and Geoanalytical Research* **34**, 11–34.

... & ... 2013. *Chinese Science Bulletin* **58**, 464–474.

... & ... 2006. *Lithos* **113**, 2–4–1.

... & ... 2010. *Chinese Science Bulletin* **55**, 1535–1546.

... 2003. *User's Manual for Isoplot 3.00: A Geochronological Toolkit for Microsoft Excel*. *Earth Science Frontier* **10**, 3–4.

... & ... 2015. *Gondwana Research*, [10.1016/j.gr.2015.04.004](https://doi.org/10.1016/j.gr.2015.04.004).

... & ... 2014. *American Journal of Science* **274**, 32–355.

... & ... 2015. *Geology* **23**, 51–4.

... 2011. *Structure of Ophiolites and Dynamics of Oceanic Lithosphere*. *Journal of Petrology* **38**, 104–114.

... & ... 200 a. *Acta Petrologica Sinica* **25**, 16–24 (in Chinese with English abstract).

... & ... 200 b. *Acta Petrologica Sinica* **25**, 14–4–1 (in Chinese with English abstract).

... & ... 2006. *Acta Petrologica Sinica* **23**, 162–174 (in Chinese with English abstract).

... & ... 2002. *Proceedings of the Ocean Drilling Program, Scientific Results, vol. 176* (eds ... & ...), 1–60. (in Chinese with English abstract).

... & ... 200 .
 ... Chinese Science Bulletin 14, 21 6 1.
 2010. ... Lithos 117, 1 20 .
 ... Journal of Asian Earth Sciences 30, 666 5.
 ... Lithos 100, 14 4 .
 2014. ... Elements 10, 101 .
 ... 2001. ... Contribution to Mineralogy and Petrology 141, 36 52.
 ... 2013. ... Gondwana Research 24, 3 2 411.
 ... Journal of Petrology 37, 6 3 26.
 ... 2013. ... Precambrian Research 231, 301 24.
 ... 2012. ... Precambrian Research 192–195, 1 0 20 .
 ... Philosophical Transactions of the Royal Society of London 335, 3 2 .
 ... 2013. ... Nature 377, 5 5 600.
 ... Nature 364, 2 30 .
 2014. ... Lithos 206–207, 234 51.
 ... 2002. ... Reviews of Geophysics 40, 3-1 3-3 .
 ... 200 .

... Science in China Series D – Earth Sciences 52, 1345 5 .
 ... Magmatism in the Ocean Basin (...), .52 4 .
 ... 200 .
 ... Chemical Geology 247, 352 3 .
 ... 200 .
 ... Acta Petrologica Sinica 23, 1 33 44 (...) .
 ... Contributions to Mineralogy and Petrology 133, 1 11 .
 ... 2006. ... Journal of Geology 114, 35 51 .
 ... 200 .
 ... Lithos 110, 35 2 .
 ... 2012. ... Earth-Science Reviews 113, 303 41 .
 ... 2006. ... Chemical Geology 20, 325 43 .
 ... 2002. ... Journal of Geology 110, 1 3 .
 ... 2006. ... Geology in China 33, 4 6 6 (...) .
 2014. ... Geoscience Frontiers 5, 525 36 .
 ... 200 .
 ... Journal of Asian Earth Sciences 32, 102 1 .
 ... 2013. ... Gondwana Research 23, 1316 41 .
 ... 2004. ... Journal of Geological Society, London 161, 33 42 .

200 a. & .
International Journal of Earth Sciences **98**, 11–21.
 & . 200 b. *American Journal of Sciences* **309**, 221–30.
 1–3. *Regional Geology of the Xinjiang Uygur Autonomous Region*. 2: 145 ().
 & . 2015. *Journal of Asian Earth Sciences* **113**, 5.
 & . 2012. *Gondwana Research* **21**, 246–65.
 & . 200 .
Chemical Geology **242**, 22–3 .
 & . 2006. *Acta Geologica Sinica* **80**, 254–63 ().
 & . 2003. *Chinese Science Bulletin* **48**, 2231–5.
 & . 2013. *Lithos* **179**, 263–4.
 & . 2012. *Journal of Asian Earth Sciences* **52**, 11–33.
 & . 200 . *Acta Petrologica Sinica* **24**, 1054–5 ().
 & . 1–6. *Annual Review of Earth and Planetary Sciences* **14**, 4–3–5–1.